ELSEVIER

Materials Characterization 58 (2007) 233–242

MATERIALS CHARACTERIZATION

The influence of surfactants on the roughness of titania sol–gel films

Jorge Medina-Valtierra [a,*], Claudio Frausto-Reyes [b], Sergio Calixto [b], Pedro Bosch [c], Victor Hugo Lara [d]

[a] *Departamento de Ingeniería Química y Bioquímica, Instituto Tecnológico de Aguascalientes, Av. A. López Mateos Ote. No. 1801, Fracc. Bona Gens, Aguascalientes 20256, Mexico*

[b] *Centro de Investigaciones en Óptica A.C., Loma del Bosque No. 115, Col. Lomas del Campestre, León, Gto. 37150, México*

[c] *Instituto de Investigaciones en Materiales, Universidad Nacional Autónoma de México, Circuito Exterior s/n, Cd. Universitaria, México, D.F. 04510, México*

[d] *Universidad Autónoma Metropolitana-Iztapalapa, Av. San Rafael Atlixco No. 186, México, D.F. 09340, México*

Received 10 March 2006; accepted 25 April 2006

Abstract

Substrate dipping in a composite sol–gel solution was used to prepare both smooth and rough thin films of titanium dioxide (TiO_2) on commercial fiberglass. The deposition of a composite film was done in a beaker using a solution of titanium (IV) isopropoxide as the sol–gel precursor and cetyltrimethyl ammonium bromide as the surfactant. In order to establish a correlation between experimental conditions and the titanium oxide produced, as well as the film quality, the calcined samples were characterized using Raman spectroscopy, UV–vis spectrophotometry, scanning electron microscopy and atomic force microscopy. One of the most important results is that a 61-nm TiO_2 film was obtained with a short immersion of fiberglass into the sol–gel without surfactant. In other cases, the deposited film consisted of a titanium precursor gel encapsulating micelles of surfactant. The gel films were converted to only the anatase phase by calcining them at 500 °C. The resulting films were crystalline and exhibited a uniform surface topography. In the present paper, it was found that the TiO_2 films prepared from the sol–gel with a surfactant showed a granular microstructure, and are composed of irregular particles between 1.5 and 3 μm. Smooth TiO_2 films could have useful optical and corrosion-protective properties and, on other hand, roughness on the TiO_2 films can enhance the inherent photocatalytic activity.

Keywords: Sol–gel deposition; Fiberglass substrate; Surfactant; TiO_2 films

1. Introduction

Metallic oxide films are solid-state systems composed of crystalline layers. Titanium dioxide (TiO_2) films are systems that may be used for many applications, mainly as photocatalytic devices. For example, Robert et al. [1] reported the effective detoxification of benzamide using TiO_2 immobilized on glass fibers. The photocatalytic activity of TiO_2 films has been determined by using methyl orange degradation [2]. Recent trends in the modification of TiO_2 films for enhancing the photocatalytic efficiency involve the incorporation of other species or surface treatments. Thus, the activity of a silane agent–TiO_2 film was tested by photodegradation of salicylic

* Corresponding author. Tel.: +52 4499105002; fax: +52 4499700423.
E-mail addresses: jormeval@yahoo.com (J. Medina-Valtierra), cfraus@cio.mx (C. Frausto-Reyes), scalixto@cio.mx (S. Calixto), croqcroqcroq@yahoo.com (P. Bosch), lacv@xanum.uam.mx (V. Hugo Lara).

1044-5803/$ - see front matter © 2006 Elsevier Inc. All rights reserved.
doi:10.1016/j.matchar.2006.04.021

acid in water [3], nanocrystalline TiO_2 thin films were examined with respect to 3, 5-dichlorophenol degradation [4], and the activity of mesoporous TiO_2 thin films was evaluated by the decomposition of acetone in air [5].

Using conventional methods, TiO_2 (anatase) films have been prepared in several ways: thin amorphous films of titania prepared by reactive evaporation [6], epitaxial films deposited by a pulsed laser deposition (PLD) technique [7], remote plasma-enhanced chemical vapor deposition of precursors such as titanium tetra-isopropoxide [8], by the utilization of a KrF laser [9] and by UV radiation [10]. More recently, novel methods have been used to obtain thin films of anatase phases on different substrates: TiO_2 deposited on glass-tubes of UV lamps by a hydrothermal method [11], amorphous TiO_2 deposited on glass beds using a plasma-CVD reactor [12], TiO_2 supported on ZSM-5 zeolite by a sol method [13], TiO_2 deposited on a flexible fiberglass cloth using different procedures [14], and transparent films deposited on polymer substrates with crystallization of sol–gel TiO_2 films at low temperatures [15]. In many studies TiO_2 films have been deposited on glass substrates using the sol–gel technique [4,16] and from the majority of these systems their photocatalytic activity was used to abate water pollution [17,18].

Fiberglass is an interesting material to be used as a support of catalytic species since it is economical, flexible, corrosion resistant and easy to handle. In this work, we have prepared TiO_2 films on fiberglass in order to generate a novel photocatalytic material. A detailed preparation process, consisting of a simple immersion method at room temperature, will be described. Moreover, differences between both smooth and rough surfaces and the effect of thickness will be related to the physical properties of TiO_2 films calcined at 500 °C. To define differences or similarities, our results are compared to already published papers. For example, porous TiO_2 films were prepared by using a sol–gel dip-coating method from an alkoxide-based solution that contained high concentrations of polyethylene-glycol [19]. The morphology of these films changed from smooth films to macroscopic cracks. However, the morphology of macropores was observed only under limited conditions. By comparing with our results, in a similar way macroscopic cracks over the film surface were observed in almost all the films.

2. Experimental methods

The thin films of TiO_2 were deposited by dip-coating in a sol–gel solution described by Wu et al. [3]. The substrates used were pieces of 8-μm fiberglass purchased from Corning Inc. Glass microscope slides were also used as substrates for reference samples. The substrates were cleaned for 2 h in an ultrasound bath with isopropanol, and then dried in an oven at 90 °C for 1 h.

The preparation procedure of TiO_2 films by the sol–gel method was as follows: 2.97 mL of titanium (IV) isopropoxide of Aldrich (TIPO) was dissolved in 30 mL of ethanol (J.T. Baker) and stirred for 1 h. In several experiments, a micellar solution was prepared by dissolving cetyltrimethyl ammonium bromide (CTAB) in 20 mL of ethanol followed by 30 min of stirring. The TIPO solution was added to the micellar solution by dripping, also followed by stirring for 30 min. Then 0.5 mL of dilute HNO_3 (in distilled water, 1/32: v/v) and 12 mL of ethanol were added to induce hydrolysis in the resultant solution. The molar composition of the starting alkoxide solution was;

$$Ti(OC_3H_7)_4 : 119C_2H_5OH : 2.70H_2O : 0.033HNO_3 : xC_{16}H_{33}(CH_3)_3N^+Br^-$$

The amount (or the factor x) of CTAB was adjusted to obtain molar ratios of CTAB to TIPO of 1/16, 1/8 and 1/4. The composite films were deposited on the glass substrates by dipping and coating them in the sol–gel solution at room temperature. The concentration of the surfactant used in the different preparations was approximately 20, 40 and 80 times the critical micelle concentrations (cmc) reported in the literature [20,21].

One sample of fiberglass was prepared without surfactant (WS), and three other samples (0.5 g each) were prepared with different [CTAB]/[TIPO] molar ratios. After the solution was prepared, the substrates were dipped in the solution for 30 s and withdrawn at a constant rate of 20 cm/min. One side of the microscope slides was covered with removable tape in order to avoid deposition on it. Coated samples were washed with distilled water and dried at ambient conditions. The substrates coated with composite films were then heat-treated at 350, 400 or 500 °C for 3 h in an air furnace. Powder samples were also prepared from the same sol–gel, which was aged at room temperature for 5 days and then dried at 120 °C in air to obtain a gel. The solid was heat-treated at temperatures between 350 and 800 °C and then ground to powder with an agate mortar.

It was found that both WS and 1/16 samples result as a thin, nearly transparent film. With a [CTAB]/[TIPO] molar ratio of 1/8 or 1/4 in the sol–gel, the composite films on the microscope slides and on the fiberglass showed a white color.

The adhesion of TiO_2 films was tested by immersing the coated fiber in a stirred ethanol bath maintained at

50 °C for 1 h. The adhesion of films on planar surfaces was tested by applying an adhesive tape and removing it abruptly [22].

The TiO_2 films deposited on fiberglass were examined using several techniques. X-ray diffraction patterns (XRD) were obtained with a Brucker 2000 diffractometer using Cu–K_α radiation (λ=1.54 Å). Preferred orientations were determined by comparing their relative intensities with those reported in the JCPDS cards [23].

Raman spectra of TiO_2 samples were obtained with a micro-Raman system using a He–Ne laser (632.8 nm) and 10 mW of power at the sample. Raman spectra were recorded with a monochromator (Jobin Yvon, HR 460) equipped with an air-cooled CCD camera as detector. Microsampling (180° backscattering configuration) was accomplished with a Zeiss 40× objective with a numerical aperture of 0.75. With this objective, the laser beam focal point diameter was ca. 2 μm. Characteristic peaks for anatase were determined by comparing their relative positions and intensities with those reported previously [24].

After dip-coating the glass substrates, residual gels were treated thermally at different temperatures. Raman spectroscopy was employed to examine crystalline structures of the resulting powders. Based on the factor group analysis and regarding the Raman active modes reported in the literature, the Raman mode characteristics for anatase and rutile are recorded in Table 1 [24,25].

A Visible Spectrophotometer (Macbeth model 7000) with a resolution of 0.1 nm was used to obtain the optical transmittance spectra and to detect absorption edges of the produced films. In order to obtain better spectra, the optical measurements were carried out on TiO_2 films deposited on microscope slides. A Film Tek 3000 SCI system was coupled to the spectrophotometer to measure film thickness. This system simultaneously solves for refractive index n (lambda), extinction coefficient k (lambda) and optimises both the reflectance and power density spectrum (FFT). A self-consistent solution is obtained by using a generalised dispersion formula to model fitted values of the dielectric function $e(l)$. Thickness determination can be done in the range of 5–550 nm with an accuracy of 6%.

The surface and pore structure of the resulting powders were analyzed using nitrogen adsorption measurements with an Accusorb 2100-E porosimeter. The titanium content of the coated fiberglass was determined by atomic absorption spectrophotometry AAS (Perkin Elmer Analyst 100) operating in the flame mode. The TiO_2 coating was dissolved by adding 0.1 g of the coated fiberglass to 5 mL of 50% HCl in deionized water (v/v). This mixture was heated at 60 °C for 30 min to completely dissolve the titanium oxides. The final solution was cooled, filtered and transferred to a 50-mL volumetric flask and diluted to volume with deionized water.

A scanning electron microscope (SEM) model JEOL 1100 was used to observe the film surface of the fiberglass. Samples were gold-coated prior to examination. Contact mode atomic force microscopy (AFM) observations of the TiO_2 films were carried out at room temperature using a Nanoscope III (Digital Instruments).

Table 1
Frequency and assignment of the Raman bands of anatase and rutile TiO_2

Phase	Frequency (cm^{-1})	In this work	Assignment	Signal
Anatase	143	138–140	B_{1g}	Very intense
	197	195–198	E_g	Very weak
	398	380–386	B_{1g}	Intense
	513	500–509	A_{1g}, B_{1g}	Less intense
	639	625–635	E_g	More intense
Rutile	144	137–138	B_{1g}	Weak
	235	223–225	c[a]	Intense
	448	430–432	E_g	Very intense
	612	592–594	A_{1g}	Very intense
	827	–	B_{2g}	Less intense

[a] Combination.

3. Results and discussion

In the sol–gel transition, the precursor powder (TIPO) dissolved in ethanol reacts with water and gives hydrolyzed Titanium (IV) isopropoxide and i-propanol. This *initial* step is the hydrolysis of the alkoxide according to Eq. (1).

$$Ti(OC_3H_7)_4 + xH_2O \rightarrow Ti(OC_3H_7)_{4-X}(OH)_X + xHOC_3H_7 \quad (1)$$

The *propagation* step is the condensation of the hydrolyzed species, with the bridging of oxygen. The chemical reaction that takes place is given by Eq. (2). Each new *alcoxolation* step is accompanied by the formation of an i-propanol molecule.

$$2[Ti(OC_3H_7)_{4-x}(OH)_x] \rightarrow Ti(OC_3H_7)_{4-x}(OH)_{x-1}] - O - Ti(OC_3H_7)_{4-x-1}(OH)_x + HOC_3H_7 \quad (2)$$

The final material before calcining has the following chemical composition, where every titanium atom is forming part of the network.

$$Ti(OC_3H_7 \text{ or } OH)_{2-y}(O)_y$$

where y can be 1 or 2.

The process is completed by the dip-coating and condensation steps to form a composite layer. A portion of surfactant can be added to give roughness and increase the thickness of the film. Moreover, the addition of surfactants to the titanium alkoxide solution can effectively lower the anatase to rutile phase transition temperature [26].

All films adhered to the glass substrate and were stable for a long period when they were kept in the ambient atmosphere. The deposited thin film undergoes solvent evaporation, solute condensation and thermal decomposition, thereby resulting in the formation of titanium dioxide films.

After calcination, every oxygen atom is bonded with a Ti atom and, hence, a pure and highly homogeneous oxide network is obtained (TiO_2). For this step, Eq. (3) is proposed when every Ti atom is surrounded by three O atoms and one –OH bond or one –OR group, into the network of the hydrolyzed gel.

$$2[\mathrm{Ti(OC_3H_7\ or\ OH)(O)}] \xrightarrow{\text{air,}>400^\circ\mathrm{C}} 2\mathrm{TiO_2} + 3\mathrm{CO_2}\uparrow + 4\mathrm{H_2O}\uparrow \quad (3)$$

Without surfactant in the sol–gel, the 61-nm thin film formed is transparent and iridescent. With a [CTAB]/[TIPO] molar ratio of 1/4 in the sol–gel, the TiO_2 remained of white colour after calcining at 500 °C and it gave a thickness of 538 nm (measured on the microscope slide).

All TiO_2 films deposited on microscope slides passed the adhesion test since they remained unchanged after removing the adhesive tape. The adhesion of the TiO_2 films to the fiberglass was considered to be good since, for all these samples, the film coating did not exhibit any peeling after washing with warm ethanol (verified with an optical microscope).

The X-ray diffraction peaks of thin films obtained without surfactant following only one immersion are not obscured by the signal from the substrate. The X-ray diffractogram of the thin film calcined at 400 °C or at 500 °C, Fig. 1, shows two well-defined 2θ peaks at 25.4° and 37.8° that correspond to a crystal with directions [101] and [112]. These data show that the film obtained under these conditions is composed of anatase (TiO_2) with a tetragonal structure (JCPDS card 21-1272). The spectrum corresponding to the film calcined at 350 °C does not show a crystalline phase for TiO_2, instead another crystalline material (peak at 29.7°) is present, and may be due to a portion of unburned TIPO. X-ray diffraction peaks corresponding to the rutile phase were not observed after this heat treatment at 500 °C.

XRD patterns corresponding to films prepared from solutions with different [CTAB]/[TIPO] molar ratios and calcined at 500 °C show different peak intensities. As shown in Fig. 2, the X-ray diffraction peaks of the calcined film prepared without surfactant (WS) are more intense than those from films prepared with surfactant. Typically, the higher the [CTAB]/[TIPO] molar ratio used in the solution, the less intense are the XRD peaks.

The average crystallite size determined with the Deybe–Scherrer equation, using the full-width-at-half-maximum values of the (101) reflection, were between 24 and 25 nm pointing out a similar crystallite size for these four samples. Differences of signal intensity are probably due to density or thickness of the film as DRX is a bulk technique.

Fig. 3 shows Raman spectra of TiO_2 films obtained from a sol–gel without surfactant or with different [CTAB]/[TIPO] molar ratios after heat-treating at 500 °C in air for 1 h. The Raman spectrum of the very thin film obtained without surfactant is not obscured by the fluorescence signal from the substrate because the laser radiation used

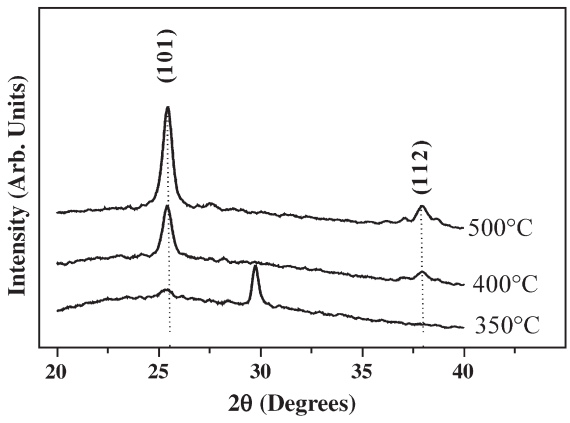

Fig. 1. XRD patterns of anatase films prepared without surfactant and calcined at different temperatures.

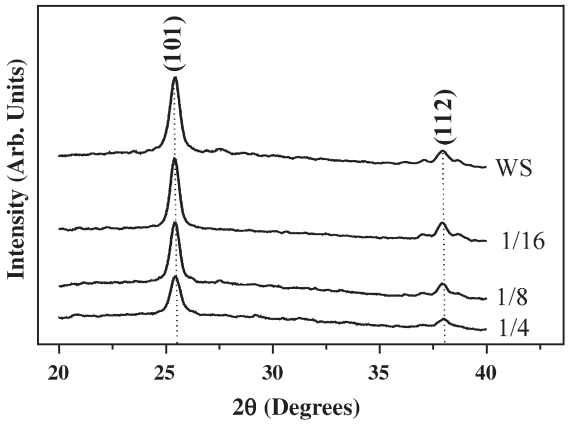

Fig. 2. XRD patterns of anatase films prepared at different [CTAB]/[TIPO] molar ratios and calcined at 500 °C.

is in the visible range. Therefore, Raman spectra obtained were not interfered with by the glass substrate. The 100–1000 cm^{-1} Raman spectra region from Fig. 3 shows four well-defined peaks at 140, 386, 509 and 633 cm^{-1}; these are assigned to the anatase tetragonal-structure in agreement with a previous report [27]. Small differences from data reported in the literature are reasonable due to the structural distortions in the thin film or by intragranular defects in samples. Raman spectra bands for rutile are reported around 144–147, 238–240, 447–448 and 610–612 cm^{-1} [28,29]. The spectrum of TiO_2 rutile, prepared from a xerogel and calcined at high temperatures, showed two main peaks at 448 and 612 cm^{-1} [29]. Therefore, in this work the stronger band around of 448 cm^{-1} was used to examine for a possible signal of rutile phase in the TiO_2 film.

The Raman spectra in Fig. 3, together with the assigned vibrational modes presented in Table 1, show that the film prepared without surfactant is a well crystallized material. TiO_2 film obtained from a sol–gel with a molar ratio of [CTAB]/[TIPO] = 1/4 shows peaks with less intensity than those obtained from a solution with a lower molar ratio. Typically, with higher amounts of surfactant in the composite films, the Raman spectra are less intense due mainly to a lower density of TiO_2 in the final film.

In other materials, a simple roughness alters the intensity of all Raman peaks in the spectrum or it can change the intensity ratio between two or more peaks [30]. In our case, the intensity from rougher films can also be reduced slightly because the surface does not act as a mirror. Moreover, the effect due to the porosity is additive because there is less matter within the irradiated volume. For example, when a sample is measured as a pellet or as powder, the intensity of its spectrum is slightly different [31].

The presence of the rutile phase was not detected in these Raman spectra since the 447 and 612 cm^{-1} peaks cannot be seen even after heat-treatment at 500 °C. This statement agrees with Djaoued et al. [32], who observed

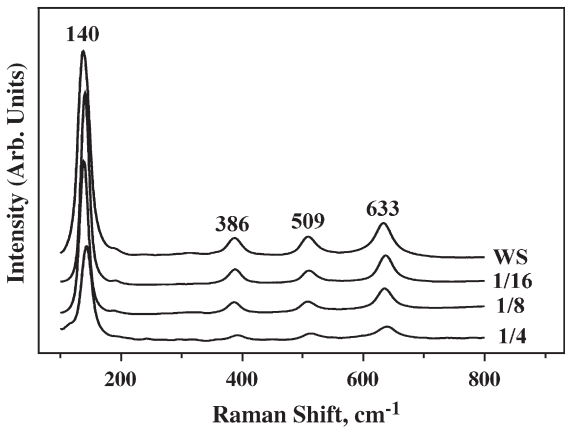

Fig. 3. Raman spectra of the TiO_2 (anatase) films calcined at 500 °C. The molar ratios of [CTAB]/[TIPO] in the sol–gel are shown for each spectrum.

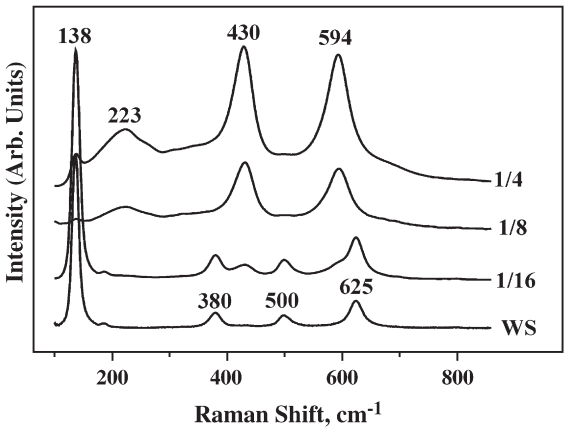

Fig. 4. Raman spectra of the TiO_2 powders calcined at 500 °C. The molar ratios of [CTAB]/[TIPO] in the sol–gel are shown for each spectrum.

only the typical bands of anatase in the spectra of TiO_2 films calcined at 700 °C. In that work a mixture of anatase and rutile phase was observed in samples treated at 800 °C, and pure rutile phase was obtained at 900 °C.

Fig. 4 shows the Raman spectra of TiO_2 powders treated at 500 °C under a static air atmosphere. For the WS sample, only the anatase phase appeared. On the other hand, for the 1/16 sample the anatase phase was accompanied by a small amount of rutile phase. Drastic changes occurred in the other more concentrated samples so that the transformation to rutile phase was achieved at a low temperature of 500 °C. In the sample with a [CTAB]/[TIPO] molar ratio of 1/4, Raman peaks of rutile phase appeared with a higher intensity due to the complete transformation of anatase. This spectrum, with peaks and bands pointing at 138, 223, 430 and 594 cm^{-1} is identical to the TiO_2 target corresponding to the rutile phase reported by Escobar-Alarcón et al. [33]. From the Raman results for TiO_2 powders, it may be concluded that the addition of the CTAB surfactant is effective in lowering the anatase-to-rutile phase transition temperature; this can be ascribed to the formation of hot zones due to combustion of the organic surfactant. The rutile phase transformation normally starts at 700 °C as observed in other TiO_2 systems [32].

Fig. 5 shows the UV–vis transmittance (T %) spectra of TiO_2 films on the microscope slides in the wavelength range of 300–800 nm. In the visible region, and specifically at 475 nm, transmittance for the TiO_2 film prepared without surfactant was 95%, while that of the microscope slide (glass substrate) was about 98%.

Transmittance values at 600 nm for the TiO_2 films were 85, 81, 78 and 67% for the samples WS, 1/16, 1/8 and 1/4. The difference in transmittance between TiO_2 films specifically in the 500–800 nm range was attributed to the difference in their film thickness, pointing out that not all the TiO_2 films are transparent. The thickness of these films is 61, 230, 315 and 538 nm, respectively. This parameter can be easily tailored by varying the withdrawal rate and the [TIPO]/[ethanol]

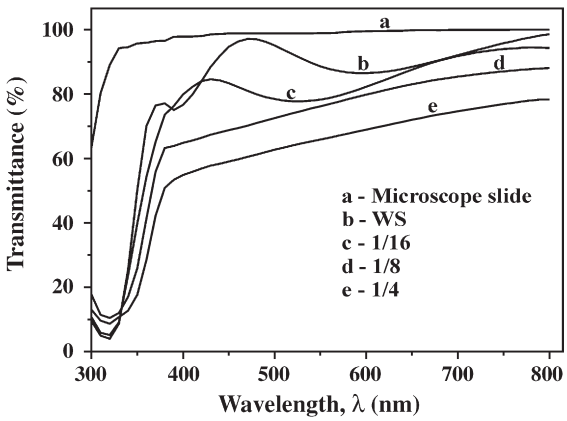

Fig. 5. Optical transmittance (T %) of the TiO_2 thin films. The molar ratios of [CTAB]/[TIPO] in the sol–gel are shown for each spectrum.

ratio in the solution. Thus, a film with a thickness greater than 60 nm can be formed without surfactant if a higher [TIPO]/[ethanol] ratio is used. A film with thickness less than 538 nm can be formed at a [CTAB]/[TIPO] ratio of 1/4 by using a shorter dip-coating time.

Note that these thickness values are much larger than the crystallite size determined by XRD. Therefore the metal oxide layer consists of several layers of crystallites which have almost the same size.

At about 380 nm the transmittance decreases quickly for all films and approaches zero at around 330 nm. This fast decrease in transmittance is due to absorption of light caused by the excitation and migration of electrons from the valence band to the conduction band of TiO_2. From Fig. 5 it is observed that the well-defined absorption edge changes slightly as the film thickness is increased.

After dissolving the TiO_2 films from the fiberglass, AAS analysis of the Ti content of each coated fiberglass mentioned above, WS, 1/16, 1/8 and 1/4, was determined to be 0.28, 0.46, 0.44 and 0.42 wt.% which is a high titanium concentration in relation to the 0.1 g fiber weight. When CTAB is added to the sol, micelles that are formed attract the species that are present in the solution, forming aggregates and therefore giving films that are thicker but less dense. This seems to be the most probable reason for the difference in wt.% Ti between the unmodified and the surfactant-modified coating and the similar Ti contents for the surfactant-modified films.

Surface areas of the TiO_2 thin films on the fiberglass could not be measured directly by the adsorption apparatus because the amount of TiO_2 was too small. Instead, surface areas of the powder samples, prepared through the same procedure as the thin films, were measured. The BET surface area of the TiO_2 powder prepared from a sol–gel with a molar ratio of [CTAB]/[TIPO]=1/4 gave a similar value (54 m^2 g^{-1}) as that of the commercial material called Degussa P-25 [27]. However, surface areas of the other TiO_2 powders were smaller than that of this commercial titania.

SEM images of the surface morphology of the TiO_2 film deposited with a molar ratio of [CTAB]/[TIPO]=1/4 on fiberglass is shown in Fig. 6. As shown on both images, the TiO_2 coating completely covers the substrate and the film exhibits a homogeneous granular surface. These grains correspond to small aggregates of crystallites as depicted by AF microscopy.

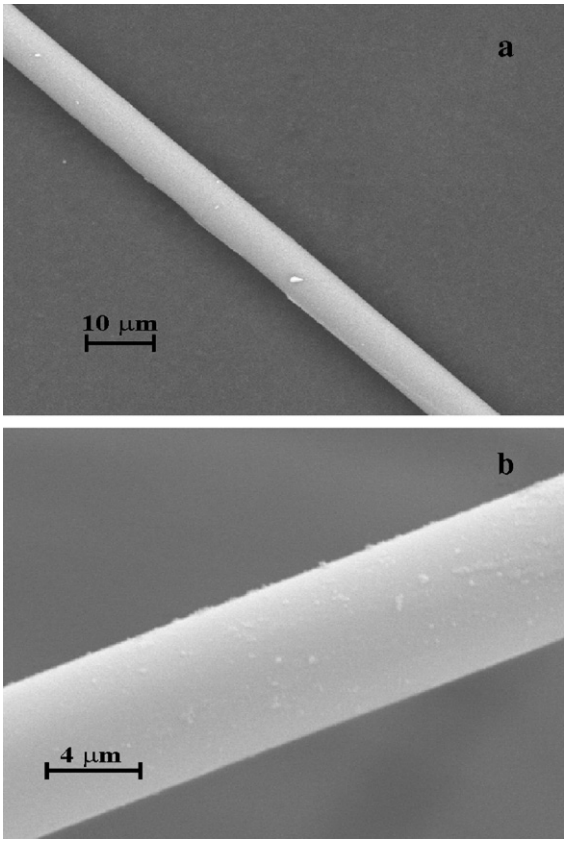

Fig. 6. SEM images of the same TiO_2 film deposited on fiberglass.

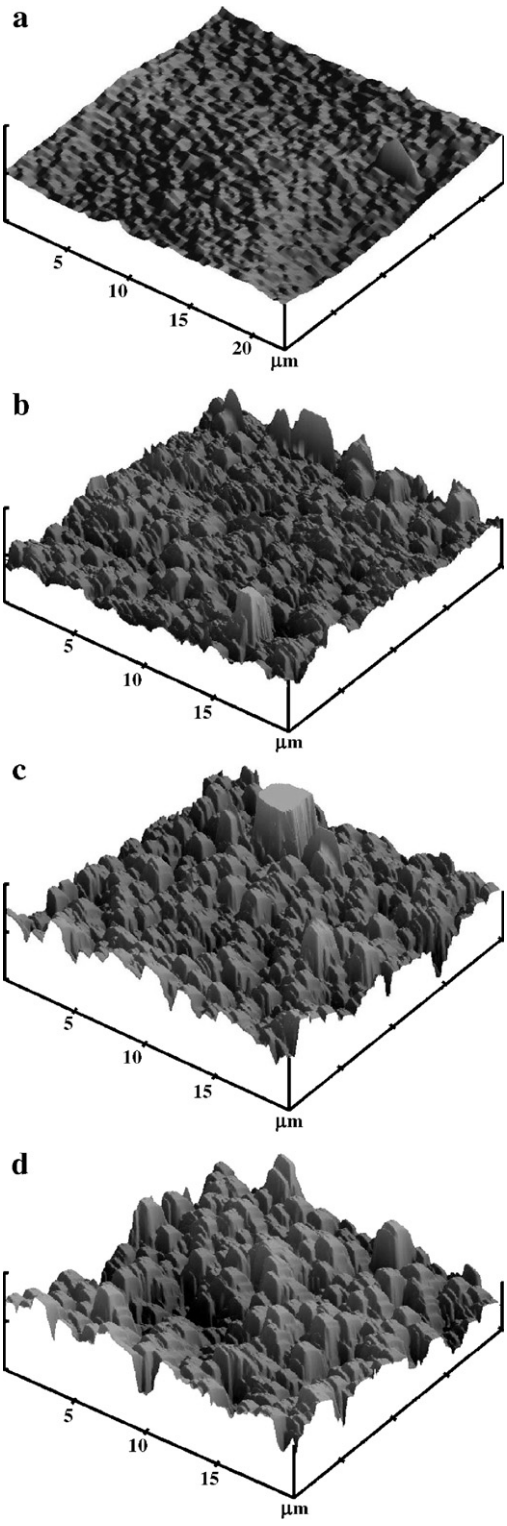

Fig. 7. (a) AFM image of the unmodified TiO_2 thin film deposited on microscope slide. AFM images of the modified TiO_2 thin films deposited on microscope slide: (b) [CTAB]/[TIPO]=1/16, (c) [CTAB]/[TIPO]=1/8, (d) [CTAB]/[TIPO]=1/4.

Table 2
Characterization features of the produced TiO_2 films and powders

Sample	Crystallite size by XRD (nm)	TiO_2 loading (mg/g)	Film thickness (nm)	Surface roughness (nm)	Powders surface area (m^2/g)
F-WS	24.0	2.87	61	0.82	<5
F-1/16	24.1	4.58	230	1.86	5
F-1/8	24.4	4.38	315	6.03	9
F-1/4	25.0	4.21	538	16.96	54

Three-dimensional AFM images of the smooth (WS) and rough TiO_2 thin films deposited on microscope slides are illustrated in Fig. 7. Low surfactant concentrations in the micellar solution promotes a mesoporosity in the resultant material [19], whereas at higher concentrations, we observe a matrix with a macroscopic domain [19] or a combination of small pores of two different sizes [21]. In this work the high roughness structure observed by AFM can be attributed to the much higher surfactant concentration used. At high surfactant concentration, a coalescence of the ordered clusters of surfactant molecules is favored to produce lamellar lattices or an unordered cluster of micelles [20]. Preparation conditions, including the thermal treatment, seem to determine the collapse of the inorganic matrix formed, which produces rough surfaces in TiO_2 coatings.

The 3D image in Fig. 7a shows that the WS sample exhibits a microgranular and flat surface. AFM investigations of this unmodified sample give a film thickness of 61 nm, and indicate that the surface roughness is about 0.82 nm. Similar roughness surfaces were reported by Yu et al. for mesoporous films [5]. The material in Yu´s work presented morphologies with a surface roughness between 0.59 and 1.06 nm. In contrast, the modified TiO_2 films, Fig. 7b–d, are rougher, forming a sponge-like structure with macroscopic cracks and thickness of 230–538 nm. In the present work, from the roughness analysis, the RMS values of the samples prepared with surfactant are between 1.86 and 16.96 nm. The physical properties of the materials are reported in Table 2.

4. Conclusions

Both smooth and rough thin anatase films were obtained with a short immersion of fiberglass into a sol–gel with or without surfactant. The deposited film consisted of a titanium precursor gel encapsulating micelles of surfactant. In all samples, the gel films were converted to the anatase phase by calcining at 500 °C.

XRD and Raman analyses carried out on the TiO_2 films showed that the films consist predominantly of the

anatase phase. Nevertheless, this also could depend on the duration of the thermal treatment. The addition of cetyltrimethyl ammonium bromide (CTAB) as a surfactant promotes the rutile phase into powders at relatively low temperature (500 °C).

By scanning electron microscopy, it was determined that all TiO_2 thin films deposited on fiberglass after a short immersion into the sol–gel were homogeneous and continuous.

By AFM technique, we found that the TiO_2 film prepared from the sol–gel with surfactant shows a granular structure, and is composed of 1.5 to about 3 μm irregular particles.

Optical sensors or semiconductor wires are potential applications of these fibers with TiO_2 films. Moreover, this novel material could be used as a catalytic material in some oxidation processes or photodegradation reactions.

Acknowledgements

The authors wish to thank Mrs. Ma. Refugio García-Ramírez for her technical support in this work. Financial support received from CONACYT (Project SEP-CONACYT-2002 No. 42168) is acknowledged.

References

[1] Robert D, Piscopo A, Heintz O, Weber JV. Photocatalytic detoxification with TiO_2 supported on glass-fiber by using artificial and natural light. Catal Today 1999;54:291–6.
[2] Yu J, Zhao X, Zhao Q. Effect of film thickness on the grain size and photocatalytic activity of the sol–gel derived nanometer TiO_2 thin films. J Mater Sci Lett 2000;19:1015–7.
[3] Wu Ch, Tzeng L, Kuo Y, Shu ChH. Enhancement of the photocatalytic activity of TiO_2 film via surface modification of the substrate. Appl Catal A Gen 2002;226:199–211.
[4] Arabatzis IM, Antonaraki S, Stergiopoulos T, Hiskia A, Papaconstantino E, Bernard M, et al. Preparation, characterization and photo-catalytic activity of nanocrystalline thin film TiO_2 catalysts towards 3, 5-dichlorophenol degradation. J Photochem Photobiol A Chem 2002;149:237–45.
[5] Yu JC, Ho W, Yu J, Hark SK, Iu K. Effects of trifluoroacetic acid modification on the surface microstructures and photocatalytic activity of mesoporous TiO_2 thin films. Langmuir 2003;19:3889–96.
[6] Mergel D, Buschendorf D, Eggert S, Grammes R, Samser B. Density and refractive index of TiO_2 films prepared by reactive evaporation. Thin Solid Films 2000;371:218–24.
[7] Yamamoto S, Sumita T, Miyashita A, Naramoto H. Preparation of epitaxial TiO_2 films by pulsed laser deposition technique. Thin Solid Films 2001;401:88–93.
[8] Nakamura M, Kato S, Aoki T, Sirghi L, Hatanaka Y. Formation mechanism for TiOx thin film obtained by remote plasma enhanced chemical vapor deposition in H_2–O_2 mixture gas plasma. Thin Solid Films 2001;401:138–44.
[9] Watanabe A, Tsuchiya T, Imai Y. Selective deposition of anatase and rutile films by KrF laser chemical vapor deposition from titanium isopropoxide. Thin Solid Films 2002;406: 132–7.
[10] Kaliwoh N, Zhang J, Boyd IW. Characterization of TiO_2 deposited by photo-induced chemical vapour deposition. Appl Surf Sci 2002;186:241–5.
[11] Lee J, Kim M, Kim B. Removal of paraquat dissolved in a photoreactor with TiO_2 immobilized on the glass-tubes of UV lamps. Water Res 2002;36:1776–82.
[12] Karches M, Morstein M, Von Rohr PR, Pozzo RL, Giombi JL, Baltanás MA. Plasma-CVD-coated glass beads as photocatalyst for water decontamination. Catal Today 2002;72:267–79.
[13] Chen J, Eberlein L, Langford CH. Pathways of phenol and benzene photooxidation using TiO_2 supported on a zeolite. J Photochem Photobiol A Chem 2002;148:183–9.
[14] Horikoshi S, Watanabe N, Onishi H, Hidaka H, Serpone N. Photodecomposition of a nonylphenol polyethoxylate surfactant in a cylindrical photoreactor with TiO_2 immobilized fiberglass cloth. Appl Catal B Environ 2002;37:117–29.
[15] Langlet M, Kim A, Audier M, Guillard C, Hermann JM. Transparent photocatalytic films deposited on polymer substrates from sol–gel processed titania sols. Thin Solid Films 2003;429:13–21.
[16] Yu J, Zhao X, Zhao Q. Effect of surface structure on photocatalytic activity of TiO_2 thin films prepared by sol–gel method. Thin Solid Films 2000;379:7–14.
[17] Zeman P, Takabayashi S. Effect of total and oxygen partial pressures on structure of photocatalytic TiO_2 films sputtered on unheated substrate. Surf Coat Technol 2002;153:93–9.
[18] Rachel A, Subrahmanyam M, Boule P. Comparison of photocatalytic efficiencies of TiO_2 in suspended and immobilised form for the photocatalytic degradation of nitrobenzenesulfonic acids. Appl Catal B Environ 2002;37:301–8.
[19] Kajihara K, Nakanishi K, Tanaka K, Hirao K, Soga N. Preparation of macroporous titania films by a sol–gel dip-coating method from the system containing poly(ethylene glycol). J Am Ceram Soc 1998;81(10):2670–6.
[20] Zhao XS, Lu GQ, Millar GJ. Advances in mesoporous molecular sieve MCM-41. Ind Eng Chem Res 1996;35:2075–90.
[21] Shyue J, De Guire MR. Single-step preparation of mesoporous anatase-based titanium–vanadium oxide and its application. J Am Chem Soc 2005;127:12736–42.
[22] Sensaki Y, Kobayashi M, Charneski LJ, Nguyen T. Chemical vapour deposition of copper thin films using new organometallic precursors with alkoxysilylolefin ligands. J Electrochem Soc 1997;144:L154–5.
[23] JCPDS Powder Diffraction File, Card 21-1272. Swarthmore, PA: JCPDS, International Centre for Diffraction Data; 1980.
[24] Xu W, Zhu S, Fu X, Chen Q. The structure of TiO_x thin film studied by Raman spectroscopy and XRD. Appl Surf Sci 1999;148:253–62.
[25] Yakovlev VV, Scarel G, Aita CR, Mochizuki S. Short-range order in ultrathin film titanium dioxide studied by Raman spectroscopy. Appl Phys Lett 2000;76(9):1107–9.
[26] Shul YG, Oh KS, Yang JC, Jung KJ. Effect of organic additive on the preparation of rutile TiO_2 by steam treatment. J Sol–gel Sci Technol 1997;8:255–9.
[27] Ohsaka T, Izumi F, Fujiki Y. Raman spectrum of anatase TiO_2. J Raman Spectrosc 1978;7:321–4.
[28] Gotic M, Ivanda M, Popovic S, Music S, Sekulic A, Turkovic A, et al. Raman investigation of nanosized TiO_2. J Raman Spectrosc 1997;28:555–8.
[29] Chang H, Huang PJ. Thermo-Raman studies on anatase and rutile. J Raman Spectrosc 1998;29:97–102.

[30] Wang A, Haskin LA, Cortez E. Prototype Raman spectroscopic sensor for in situ mineral characterization on planetary surfaces. Appl Spectrosc 1998;52:477–87.
[31] Haskin AL, Wang A, Rockow KM, Jolliff BL, Viskupic RL. Raman spectroscopy for mineral identification and quantification for in-situ planetary surface analysis: a point count method. J Geophys Res 1997;102:19,293–306.
[32] Djaoued Y, Badilescu S, Ashirt PV, Robichaud J. Vibrational properties of the sol–gel prepared nanocrystalline TiO_2 thin films. Int J Vibr Spec 2002;5(6):4–15.
[33] Escobar-Alarcón L, Haro-Poniatowski E, Camacho-López MA, Fernández-Gausti M, Jiménez-Jarquín J, Sánchez-Pineda A. Structural characterization of TiO_2 thin films obtained by pulsed laser deposition. Appl Surf Sci 1999;137:38–44.